

Figure 1. SAW delay line consisting of two interdigital transducers on a piezoelectric substrate.

ACOUSTIC MICROWAVE DEVICES

Since the first experiments on piezoelectricity by the Curie brothers in 1880, ultrasonic devices of many forms have been used to process electrical signals. Bulk crystal resonators, in particular, have proved to be compact and reliable, and they have become ubiquitous in high-precision oscillators having a fundamental frequency of up to 20 MHz. At higher frequencies the bulk crystal resonators must be very thin, so they are too fragile for most applications.

In 1965 White and Voltmer demonstrated that it was possible to generate, propagate, and detect mechanical waves on the surface of a piezoelectric crystal (1). Their invention overcame the frequency limitations of the bulk crystal resonators because the frequency of operation became independent of the crystal thickness. It also made the mechanical waves accessible at arbitrary points on the surface, thus permitting multiple sampling of the wave.

Since the velocity of ultrasonic waves in crystals is in the order of 10^5 times lower than the velocity of electromagnetic waves, ultrasonic microwave circuits are extremely compact. For a given substrate, the behavior of an ultrasonic device is determined by the structure of its transducers, which are designed by well-developed procedures.

These characteristics have been extensively exploited over the past three decades, and the devices, generically known as surface acoustic wave (SAW) devices, have led to major advances in pulse compression radar and have become a critical enabling technology for the wireless communications industry.

SAW DEVICE STRUCTURES

Delay Line

A SAW delay line is illustrated in Fig. 1 and is the simplest device of its type. It consists of two thin-film metallic trans-

ducers placed on the surface of a piezoelectric substrate. Common substrates are listed in Table 1. The transducers are usually created using a single-step photolithographic process; they are made of a light metal such as aluminum so that the effect of their mass on the substrate is minimized. The photolithographic resolution in the fabrication process limits the frequency of operation of SAW delay lines, where an achievable line width of $0.5 \mu\text{m}$ would limit the frequency of operation to less than 2 GHz. For systems that operate at higher frequencies, either the devices must be built using more expensive electron beam lithography or the signals must be down-converted to an intermediate frequency (IF) before being applied to the SAW device.

The principal benefit of employing SAW delay lines is the large group delays that are possible. For example, a device having a distance (center to center) between transducers of 0.5 cm would produce a delay in the order of $1.5 \mu\text{s}$. In addition, since the wave velocity is frequency independent, this delay applies to all frequency components that the device supports.

The structure of the transducers varies, but the most common type by far is the interdigital transducer (IDT). The IDT consists of an array of parallel strips (“fingers”) of alternating polarity. When a RF signal is applied to the input IDT, the electric fields between the metal strips induce mechanical deformations that propagate as waves in the crystal. These waves generate an electric potential between the strips in the output IDT that produces a current in the load.

The frequency response of the device can be estimated by recognizing that a modulated pulse can approximate the im-

Table 1. Common Substrates Used in Surface Wave Devices

| Crystal | Cut | ν (m/s) | k^2 (%) | Temperature Coefficient (ppm/K) |
|-------------------|----------------|-------------|-----------|---------------------------------|
| Quartz | ST-X | 3158 | 0.116 | 0 |
| Lithium Niobate | Y-Z | 3488 | 4.82 | +94 |
| Lithium Niobate | 128° -X | 3992 | 5.44 | +75 |
| Lithium Tantalate | Y-Z | 3230 | 0.66 | +35 |

Source: Morgan (14).

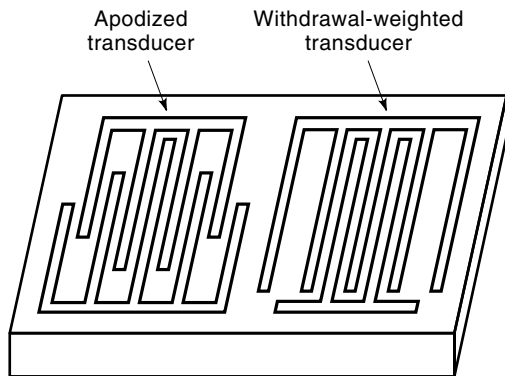


Figure 2. SAW device employing an apodized transducer and a withdrawal-weighted transducer to control its frequency response.

pulse response of each IDT. The frequency response for a device having two identical transducers is thus

$$|H(f)| \approx A \left| \frac{\sin[N\pi(f - f_0)/f_0]}{N\pi(f - f_0)/f_0} \right|^2 \quad (1)$$

where A is a constant and N is the number of finger pairs in each transducer. The device's center frequency f_0 given by

$$f_0 = \frac{v}{p} \quad (2)$$

Here v is the acoustic wave phase velocity in the transducer region and p is the finger periodicity, as shown in Fig. 1.

The insertion loss of a SAW filter is often high. Since both IDTs are bi-directional three-port (one electrical, two acoustic) devices, each IDT will contribute an inherent 3 dB loss (6 dB in total) when the two electrical ports are matched to the source and load, respectively. This matched condition unfortunately also results in the maximum level of acoustic wave regeneration by each IDT and leads to severe multipath interference known as triple-transit interference (TTI). Consequently most SAW devices are intentionally mismatched at the electrical ports so that acoustic regeneration is reduced. An insertion loss of between 20 dB and 30 dB is common.

The frequency response of physical delay lines usually exhibits several other distortions attributed to second-order effects. The dominant effects are direct electromagnetic coupling ("feedthrough") between input to output transducers, reflections from electrode edges, acoustic beam diffraction, and bulk wave interference.

Transversal Filter

The transversal filter is a generalization of the delay line in which the relative effect of individual IDT fingers is varied so that the frequency response of the transducer can be controlled. The control is commonly achieved either by apodization, which consists of varying the finger lengths, or by withdrawal weighting, which involves selectively removing fingers. These techniques are illustrated on the device shown in Fig. 2.

In a first-order design process, each finger (or each finger overlap) in an IDT is represented by a delta function whose magnitude is proportional to the length. The impulse re-

sponse of the IDT is then a sequence of weighted delta functions separated by $\tau = p/2v$ seconds. This representation is identical to the one commonly used in the design of finite impulse response (FIR) digital filters for which there are extensive design tools. The most common of these tools is the Remez exchange algorithm, for which computer programs are readily available (2), but other optimization algorithms can also be used. Once the equivalent digital FIR filter has been designed, the SAW filter is obtained by making the finger lengths (or finger overlaps) proportional to the tap weights of the digital filter. If the transducer has an impulse response that is symmetrical, then its frequency response will exhibit a linear phase. This property is important in communications applications.

Care must be exercised when designing a SAW filter having two apodized transducers. Since in this case the acoustic beam generated by the first apodized transducer will not be uniform across its width, the signal detected by each finger (or finger overlap) in the second transducer will not in general be proportional to its length. Because of the difficulties that this behavior introduces in the design process, the second transducer is usually not apodized.

Dispersive Delay Line

Both the SAW delay line and transversal filter are usually designed to have a linear phase response. There are situations, however, where a nonlinear phase response is desirable. For example, a frequency-modulated ("chirp") impulse response is often used to improve the range and resolution of radar systems.

A dispersive SAW device can be made by varying the finger positions of a delay line. Alternatively, grooves of varying periodicity can be etched into the substrate, as shown in Fig. 3, to create a reflective array compressor (RAC) (3). The various frequency components in the acoustic beam will be reflected efficiently in the region where the grooves have a periodicity equal to half the acoustic wavelength. The frequency components will thus travel different distances and will reach the

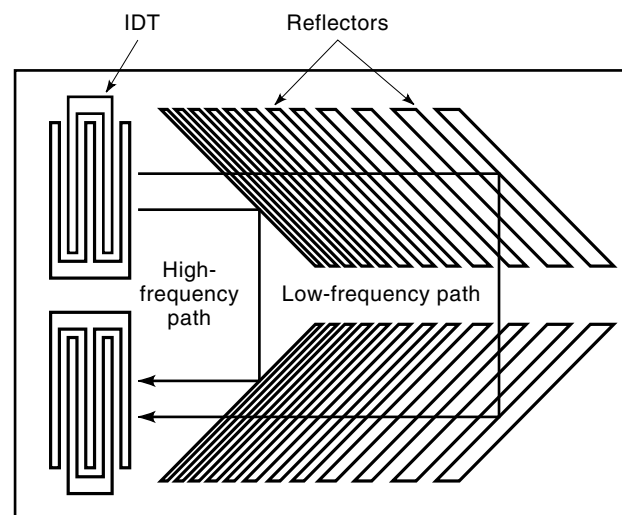


Figure 3. Reflective array compressor (RAC) which introduces signal dispersion by imposing a different signal path on each frequency component.

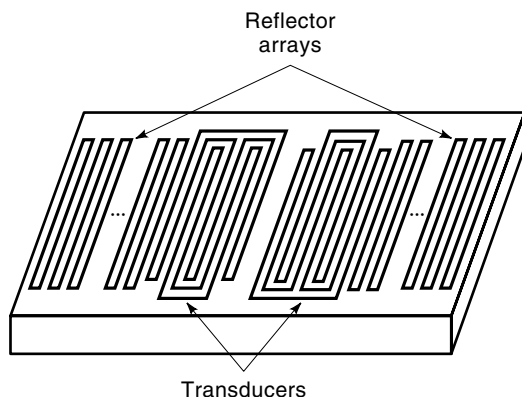


Figure 4. SAW resonator with reflector arrays to trap acoustic energy over a narrow frequency range.

output transducer with differing delays. The phase response of the filter is obtained by integrating the radian frequency with respect to time, so a nonconstant delay will produce the desired nonlinear frequency response.

Single-Mode Resonator

An array of metal strips or grooves on the surface of the substrate can reflect SAW energy. If we place such arrays on the far sides of a two-transducer device as shown in Fig. 4, we can create an acoustic resonant cavity. Resonance will occur and the acoustic energy will be trapped in the cavity when the acoustic wave has a wavelength that is approximately equal to an even multiple of the strip periodicity.

When properly designed, a SAW resonator can achieve a quality factor, measured as the inverse of the fractional bandwidth, equal to about 10,000. In addition the SAW resonator does not suffer from high insertion loss because the acoustic energy is trapped in the cavity and does not get dissipated in the substrate. An insertion loss of less than 2 dB is easily achievable.

Multimode Resonator

If we allow the acoustic energy in two identical resonant cavities to couple, the resonant frequency of the combined structure will split into two resonant frequencies. This property is often used to produce resonators that exhibit a higher fractional bandwidth than single-cavity resonators while still maintaining their low insertion loss.

The resonators can be longitudinally coupled, in which case two cavities are placed in line and the reflector array that they share is shortened to allow the acoustic energy to “leak” into the adjacent cavity. This approach allows the designer to precisely control the coupling between the cavities. Alternatively, the cavity length can be increased sufficiently to permit two or more modes to exist within the single cavity. However, at frequencies not reflected by the reflector arrays, the SAW waves will be able to freely propagate between transducers in these structures. This leads to poor out-of-band rejection.

The resonators may also be transversely coupled. In this case the acoustic cavities are placed in parallel, with a very narrow gap (usually a grounded metal strip) between them. Acoustic energy is coupled between the cavities through the

evanescent “tail ends” of the transverse energy distribution of each cavity. This approach gives very limited control over the coupling between cavities, but leads to excellent out-of-band rejection, in the order of 60 dB.

Low-Loss Structures

The previous paragraphs have described traditional SAW devices, which can be divided into high-loss filters with outstanding frequency response characteristics and low-loss narrowband resonant devices with responses over which the designer has limited control. Over the past few years, a new class of device has emerged that can provide both low loss and control over the shape of the frequency response.

Designing transducers that generate acoustic energy primarily at one port can reduce the insertion loss. This is done by introducing wave reflections, within each IDT, that add in phase with waves propagating in the desired direction but that add out of phase with waves propagating in the opposite direction. Since the standard IDT is symmetric, it cannot generate unsymmetrical output. We must employ instead transducers that have multiple electrodes, often of varying width, per period. Several examples of structures employing single-phase unidirectional transducers (SPUDT) are given in (4). These devices require higher photolithographic resolution, and their fabrication presents severe difficulties at frequencies above 1 GHz.

A second approach to reducing the insertion loss is to employ multiple bi-directional transducers that are alternatively connected to the input and output ports. Since each input transducer (except if located at the ends) has a receiving transducer at both acoustic ports, and since each output transducer (except if located at the ends) has a transmitting transducer at each port, very little acoustic energy is lost. These devices, known as interdigitated interdigital transducers (IIDT), are not subject to the same fabrication limitations at high frequencies as the devices described in the previous paragraph, but they often exhibit severe ripples in the frequency response.

APPLICATIONS

Nyquist Filter

Consider a communication system designed to transmit digital bits (assume that each bit is transmitted as a delta function for now) every T seconds. The frequency response of the transmitted information must be restricted to the available channel bandwidth, which makes the impulse response of the received bits infinite in length. Unless special steps are taken, successive bits will produce intersymbol interference (ISI).

To minimize this interference, it is important that the channel’s impulse response exhibit a very small value at all sampling instances $t = nT$, $n \neq 0$. A channel with an ideal rectangular frequency response and a bandwidth of $BW = 1/T$ Hz would have a sinc impulse response,

$$\text{sinc}\left(\frac{t}{T}\right) = \frac{\sin(\pi t/T)}{\pi t/T} \quad (3)$$

which has the desired property. There are other functions, such as the “raised-cosine” function (5), that have the same

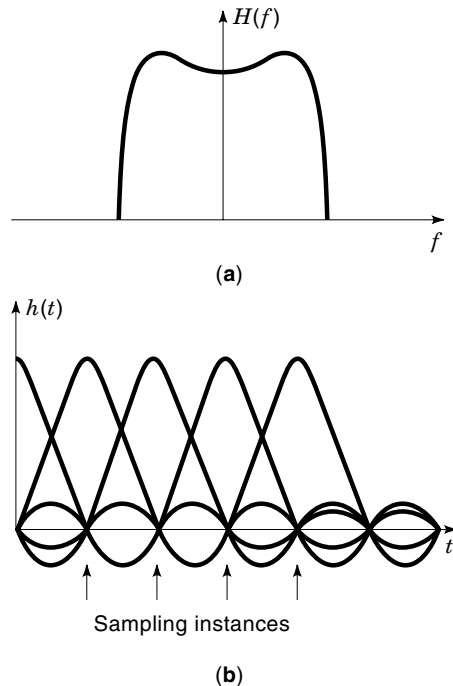


Figure 5. (a) Raised-cosine Nyquist filter frequency response showing predistortion corresponding to response of transmitted bit; (b) very small impulse response of the bit at sampling instances corresponding to neighboring bits.

property. Any deviation from such frequency responses by the channel filter will quickly degrade the performance of the system.

The frequency response of the channel filter must be modified to account for the frequency response of the transmitted bit, which in practice cannot be a true delta function. If we assume a rectangular bit (with its sinc-shaped frequency response), a corresponding 1/sinc response must be superimposed on the frequency response of the filter. The resulting frequency response, and its time-domain properties, are illustrated in Fig. 5.

Because of their performance, reproducibility, and their ability to operate at intermediate frequencies (so that a single filter can operate on the combined in-phase and quadrature channels instead of requiring a baseband filter for each of these channels), SAW filters are often used in these applications (6).

Satellite Subchannels

Satellites usually have several transponders, and these are often leased to users. For example, the standard bandwidth of a C-band (6/4 GHz) satellite channel is 40 MHz, of which 36 MHz is usable because of the required guard bands between channels. In a conventional system the user must lease the entire channel, whether or not the bandwidth is needed. The high cost of leasing the entire channel can be a major deterrent.

The high selectivity of SAW filters makes it possible to divide the satellite channel into three or more subchannels, possibly of varying bandwidth. Furthermore, if the magnitude and phase of these filters are carefully controlled, it is possi-

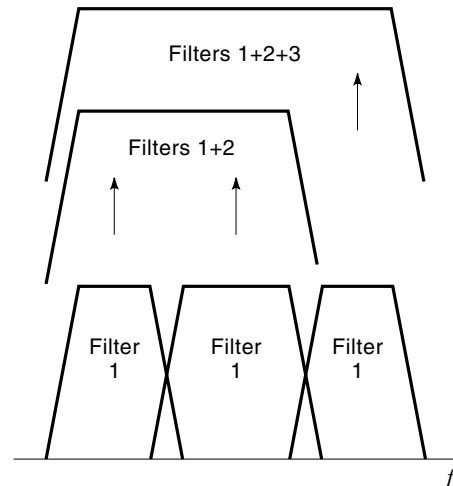


Figure 6. Filters in a SAW filter bank seamlessly combined to dynamically vary a channel bandwidth.

ble to combine two or more of these subchannels to form a contiguous channel of higher bandwidth, up to the bandwidth of the transponder. Such a system is illustrated in Fig. 6. The INMARSAT 3 satellite uses this type of system to service its mobile users (7).

An added benefit of employing SAW filters instead of the more conventional microwave cavity filters is their higher selectivity. This increases the usable satellite channel bandwidth because guard bands can be narrower.

Wireless Communications

Wireless communications systems require inexpensive, rugged, and compact components that consume very little power. Low-loss SAW devices excel in all four attributes and have been widely adopted by all major manufacturers (8).

SAW longitudinally coupled resonator filters are often used in the front-end to remove out-of-band signal interference. A waveguide-coupled resonator filter is then used to select the desired channel. Figure 7 illustrates the uses of SAW components in a cellular telephone.

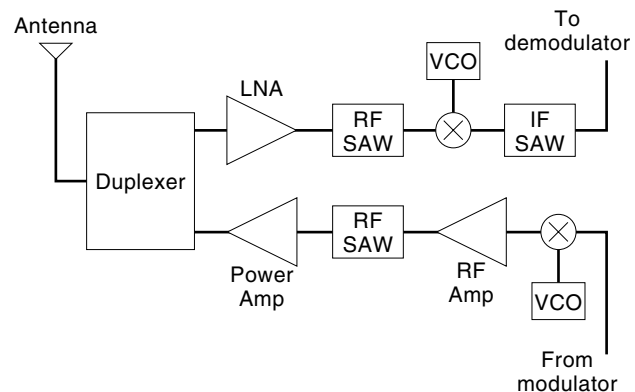


Figure 7. Block diagram of cellular telephone showing a wide bandwidth RF SAW device to remove out-of-band signals and a narrow bandwidth IF SAW device to select the individual channel.

Oscillators

Stable oscillators require a narrowband device in their feedback path whose passband frequency can be precisely established. The frequency response of the device should also present a low insertion loss and be highly stable. Finally, for volume applications, the response must be easily reproducible.

SAW resonators meet all of these requirements, and they are lightweight and rugged. When compared to other technologies, they can be manufactured at a low cost. For these reasons SAW oscillators are widely used whenever signals in the 50 MHz to 2 GHz range are required.

Oscillator stability is usually categorized as either short or long term. Short-term stability refers to output frequency variations lasting less than 1 second, and which are caused by random thermal vibrations and by the discrete nature of electric charge. Long-term stability encompasses effects due to temperature variations and component aging.

Short-term stability can be improved by selecting a high-Q feedback filter, an amplifier with low flicker noise and noise factor, and a clean power supply. In the case of SAW oscillators, it is also important to isolate the SAW device from mechanical vibrations, since the piezoelectric substrate can convert them to electrical signals. Short-term stability is usually measured in terms of single-sideband phase noise, which describes the oscillator output power density, normalized to the power of the carrier, at specific offset frequencies. A 500 MHz SAW oscillator, for example, is typically able to achieve phase noise levels of -130 dBc/Hz at 1 kHz offset from the carrier (dBc refers to decibels with respect to the carrier). The phase noise then typically drops to about -175 dBc/Hz at 100 kHz offset and then levels off (9).

Long-term stability can be improved by placing the oscillator in a temperature-controlled environment. Placing the SAW device in a package with thermal characteristics that are similar to those of the substrate also helps reduce mechanical stresses. Because component aging occurs predominantly in the early stages, it is also important to “burn-in” all oscillator components by subjecting them to high signal levels and high temperatures for an extended period of time. SAW oscillator long-term stability is usually measured in parts per million (ppm), and a good design can achieve 1 ppm per year at a fixed temperature or about 20 ppm over a temperature variation of 50 K.

Chirp Fourier Transformer

The SAW chirp Fourier transformer is an analog circuit that is able to perform a finite bandwidth windowed Fourier transform. The circuit is based on a simple algebraic manipulation of the formula for the Fourier transform $S(\omega)$ of a time signal $s(t)$:

$$S(\omega) = \int_{-\infty}^{\infty} s(t)e^{-j\omega t} dt \quad (4)$$

Substituting $-2\omega t = (t - \omega)^2 - t^2 - \omega^2$ and then $\omega = \mu t$, we obtain

$$S(\omega) = S(\mu t) = \exp\left(-j\frac{\mu}{2}t^2\right) \int_{-\infty}^{\infty} \left[s(\tau) \exp\left(-j\frac{\mu}{2}\tau^2\right) \right] \times \exp\left[j\frac{\mu}{2}(t - \tau)^2\right] d\tau \quad (5)$$

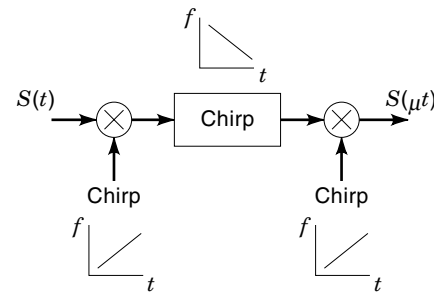


Figure 8. A multiply-convolve-multiply (MCM) SAW Fourier transformer which has a time-domain output that is a scaled version of the input signal's frequency response.

This expression can clearly be represented by the circuit shown in Fig. 8, which involves a multiplication by a linear frequency-modulated (FM) signal followed by a convolution with another FM signal having a frequency variation opposite to the first. The output of the convolver is then multiplied by a third FM signal having the same variation as the first. A similar transformation can show that the dual circuit, consisting of a convolve-multiply-convolve system, produces the same result.

In a practical system the convolutions are performed by feeding the signal to a SAW chirp filter having a linear group delay. The multiplying signals can be provided by impulsing SAW chirp filters but are usually generated digitally because this approach makes it easier to compensate for imperfections in the convolving SAW chirp filters.

To the author's knowledge, the SAW chirp Fourier transformer has not been widely used in any commercial applications. Studies have shown, however, that it could be very competitive in key communications satellite applications (10).

SUBSTRATES

There are currently many substrates in use for SAW devices. The most common are lithium niobate (LiNbO_3), quartz, and lithium tantalate (LiTaO_3), which are cut at various angles to the crystalline axes. Table 1 summarizes the most important properties of some of the more common crystal cuts.

The phase velocity v of the wave, combined with the photolithographic resolution of device fabrication process, determine the maximum sampling frequency of the transducers. Clearly, since IDT electrodes must be at most half a wavelength apart, a high velocity is desirable at microwave frequencies.

The coupling coefficient k^2 provides an indication of the electromechanical coupling efficiency. It is computed by evaluating the fractional velocity difference between waves propagating under metallized and free surfaces. Filters built on substrates with a higher k^2 can achieve lower insertion loss and wider bandwidths.

The temperature coefficient determines the effect of temperature changes on the acoustic phase velocity. This parameter is particularly important in oscillator applications where the cost of controlling the substrate temperature is excessive.

In general, LiNbO_3 crystals are used for wideband devices such as transversal filters, where the device may be placed in a temperature-controlled environment, or where small pass-

band shifts due to temperature variations are of minor concern. Quartz is usually preferred for narrowband applications, such as for resonators to be used in oscillators where minor frequency shifts due to temperature variations are of major concern. The ST-X cut of quartz, with its zero first-order temperature coefficient at room temperature, is ideal for this type of application.

LiTaO₃ is often selected as a compromise between the two other substrates. Its temperature coefficient is lower than that of LiNbO₃, but its coupling coefficient is higher than for quartz.

ACOUSTIC MODES

A solution to the acoustic wave propagation in a piezoelectric substrate requires that both Maxwell's and Newton's equations be solved simultaneously in a nonisotropic medium. Maxwell's equations give us

$$\nabla \cdot D = \rho_s \quad (6)$$

and

$$E = -\nabla\phi \quad (7)$$

where D is the electric flux density, E is the electric field, ρ_s is the surface charge density, and ϕ is the potential. Newton's equations state that

$$\sum_j \frac{\partial T_{ij}}{\partial x_j} - \rho \frac{\partial^2 u_i}{\partial t^2} = 0 \quad (8)$$

where T_{ij} is the stress, ρ is the substrate density, and u_i is the particle displacement in the x_i direction. Strain is defined as

$$S_{ij} = \frac{1}{2} \left(\frac{\partial u_i}{\partial x_j} + \frac{\partial u_j}{\partial x_i} \right) \quad (9)$$

The Maxwell and Newton equations are coupled through the piezoelectric equations

$$T_{ij} = \sum_k \sum_l c_{ijkl}^E S_{kl} - \sum_k e_{hij} E_k \quad (10)$$

$$D_i = \sum_k \sum_l e_{ikl} S_{kl} + \sum_k \epsilon_{ik}^S E_k \quad (11)$$

where c_{ijkl}^E values are the elastic tensor components for the specific substrate, e_{ikl} are the piezoelectric tensor components, and ϵ_{ik}^S are the permittivity tensor components.

The wave solutions obtained by solving the above equations, subject to boundary conditions, can be classified by their propagation properties. The most common types are bulk waves, surface acoustic waves, surface transverse waves, and leaky waves.

Bulk Waves

Bulk acoustic waves are waves that propagate in the interior of the substrate, so they are not subject to the substrate boundary conditions. A bulk wave will have a particle motion that is composed of a fast longitudinal wave component,

whose particle motion is in the same direction as the wave, and two slower transverse wave components, whose particle motions are perpendicular to the wave. The latter are usually termed fast shear and slow shear waves, owing to their different phase velocities. In a piezoelectric substrate all of these wave components will have phase velocities that depend on the propagation direction of the bulk wave.

Surface Acoustic Waves

Surface acoustic waves satisfy the Maxwell and Newton equations in a piezoelectric half-space. Their motion is retrograde elliptical, and their velocity is lower than that of slow shear waves. This slow velocity leads to very low propagation losses because it precludes energy-robbing coupling between SAW and any bulk waves. The acoustic energy is also confined to within about 1 wavelength of the surface, which makes it easily accessible.

For specific substrates the particle motion of the surface wave is entirely in the sagittal plane (defined by axes x_1, x_3 in Fig. 1), and the waves are then referred to as pure Rayleigh waves.

Bluestein-Gulyaev Waves

Bluestein-Gulyaev waves, also called surface transverse waves (STW), only contain particle motion in the x_2 direction and can be generated with the traditional IDT structure. In general, the energy will propagate at a nonzero angle to the surface, which makes the wave lossy. However, if the surface is subjected to a periodic stress, the STW can be guided parallel to the surface so that it behaves very much like a SAW, and it is then called a surface-skimming bulk wave (SSBW). IDTs or reflector arrays build with a heavier or more metal are usually used to guide the wave.

For particular substrate cuts, STW or SSBW can be the dominant acoustic mode. The waves resemble shear horizontal waves and have a higher velocity than surface waves. Because of this higher velocity, devices using STW/SSBW are sometimes used instead of their SAW counterparts at high frequencies.

Leaky Waves

For some substrates a SAW cannot satisfy the boundary conditions. Instead, a faster pseudo-SAW, also referred to as a leaky wave, exists in which the propagating acoustic energy leaks slowly into the substrate. The coupling coefficient of leaky waves can be higher than that of a SAW, and its temperature coefficient for some crystal cuts can be almost zero. For these reasons leaky waves are being increasingly used, particularly at high frequencies.

DEVICE MODELS

Attempts to accurately model surface wave devices have met with varying success. The electromechanical interactions that are central to their operation require that both Maxwell's and Newton's equations be solved for the given boundary conditions. Until recently the computational requirements to fully model even the simplest devices have been excessive. As a result varying levels of simplification have been adopted in order to generate useful design tools. Effects that have not

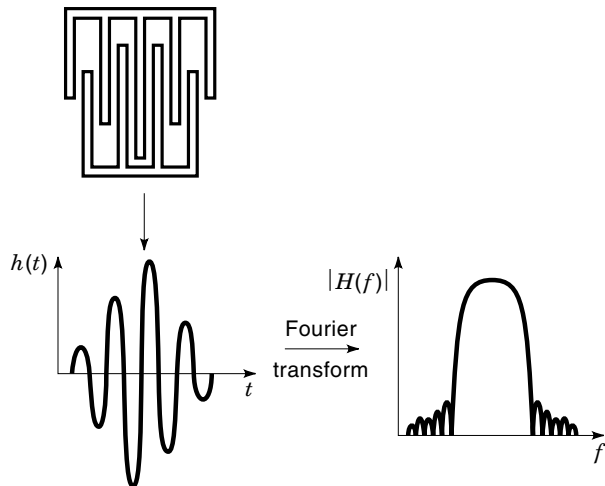


Figure 9. Impulse response model of a transducer obtained by replacing each finger overlap by a scaled half cycle of a sine wave.

been predictable with these simplified models have been dismissed as “second-order effects,” with several techniques used to minimize their effect on the desired behavior of the device (11).

Impulse Response Model

The impulse response model was first derived by Hartmann, Bell, and Rosenfeld (12) as an alternative to more complicated equivalent circuit approaches. It provides more information on a SAW device’s performance than the delta function model described by Eq. (1) because it includes information on electrical impedances and can cater to transducers with nonuniform electrode spacing.

The process of modeling a SAW device with the impulse response model involves three steps: First, each electrode overlap is replaced with a half cycle of a sine wave whose magnitude is proportional to the length of the overlap. Second, if electrode spacing is not uniform, then the magnitude of each i th half cycle is further scaled by $f_i^{3/2}$, where f_i is the instantaneous frequency at that point in the transducer. Third, the frequency response is obtained by taking the Fourier transform of the resulting impulse response. The technique is illustrated in Fig. 9.

The input impedance of a transducer can be computed from the impulse response model through energy conservation arguments. The equivalent circuit consists of a radiation conductance, representing acoustic energy generation, in parallel with a radiation susceptance, corresponding to energy absorption and regeneration in the transducer, and with a static capacitance. The radiation conductance of an IDT with uniformly spaced electrodes is found to be

$$G_a(f) = 8k^2 C_s f_0 N^2 \left| \frac{\sin[N\pi(f - f_0)/f_0]}{N\pi(f - f_0)/f_0} \right|^2 \quad (12)$$

while the radiation susceptance is the Hilbert transform of $G_a(f)$ and is given by

$$B_a(f) = 8k^2 C_s f_0 N^2 \frac{\sin[2N\pi(f - f_0)/f_0] - 2N\pi(f - f_0)/f_0}{2[N\pi(f - f_0)/f_0]^2} \quad (13)$$

The static capacitance for the transducer is

$$C_t = NC_s \quad (14)$$

In Eqs. (12) through (14), k^2 is the electromechanical coupling constant, C_s is the capacitance per finger pair, and N is the number of finger pairs in the transducer. The equivalent circuit values for transducers with nonuniformly spaced electrodes can be found in (12).

Coupling-of-Modes Model

The coupling-of-modes (COM) model is a phenomenological description of the behavior of propagating waves that are subjected to a periodic disturbance in their propagation medium. The technique is ideally suited to the computation of the behavior of SAW structures that contain a large number of equally spaced electrodes or reflector strips. The COM approach is very numerically efficient but is only accurate over fractional bandwidths of about 10%. It also must be slightly modified to model devices that employ leaky waves.

Consider two counterpropagating waves having complex amplitudes $w^+(x)$ and $w^-(x)$, propagating in the forward and backward directions, respectively, in a transducer region. Because of reflections and acoustic generation at the electrodes, these waves will be coupled so that

$$\begin{aligned} \frac{\partial w^+(x)}{\partial x} &= -j\delta w^+(x) + j\kappa w^-(x) + j\alpha V \\ \frac{\partial w^-(x)}{\partial x} &= j\delta w^-(x) - j\kappa^* w^+(x) - j\alpha^* V \\ \frac{\partial I(x)}{\partial x} &= -2j\alpha^* w^+(x) - 2j\alpha w^-(x) + j\omega C_0 V \end{aligned} \quad (15)$$

where κ is the distributed reflection coefficient, α is the distributed transduction coefficient, V is the applied voltage, ω is the radian frequency deviation from the Bragg frequency given by

$$\delta = \beta - \frac{\pi}{a} \quad (16)$$

where β is the propagation constant and a is the electrode separation. The terms containing V and the equation for the incremental current $I(x)$ can be disregarded when dealing with reflector arrays.

If we write Eq. (15) in matrix form, we obtain

$$\begin{aligned} \frac{\partial w(x)}{\partial x} &= Cw(x) + fV \\ \frac{\partial I(x)}{\partial x} &= Nw(x) + j\omega C_0 V \end{aligned} \quad (17)$$

where

$$w(x) = \begin{bmatrix} w^+(x) \\ w^-(x) \end{bmatrix}, \quad C = \begin{bmatrix} -j\delta & j\kappa \\ -j\kappa^* & j\delta \end{bmatrix}, \quad f = \begin{bmatrix} j\alpha \\ -j\alpha^* \end{bmatrix}, \quad \text{and} \\ N = \begin{bmatrix} -2j\alpha^* & -2j\alpha \end{bmatrix}$$

The general solution for the waves is

$$w(x) = V_e E(x) V_e^{-1} w(0) + (V_e E(x) V_e^{-1} - II) C^{-1} f V \quad (18)$$

where V_e is the 2×2 matrix containing the eigenvectors of C in its columns. II is the 2×2 unit matrix, and

$$E(x) = \begin{bmatrix} e^{\lambda_1 x} & 0 \\ 0 & e^{\lambda_2 x} \end{bmatrix} \quad (19)$$

for which λ_1 and λ_2 are the eigenvalues of C (13). In the case of transducers, the solution requires an expression for the current, which is obtained by integrating the incremental current over the length of the transducer. For a transducer of length x , we get

$$I = NV_e \Lambda^{-1} (E(x) - II) V_e^{-1} w(0) + \{N[V_e \Lambda^{-1} (E(x) - II) V_e^{-1} + xII] C^{-1} f + j\omega C_t\} V \quad (20)$$

where $C_t = xC_0$ is the total static capacitance of the transducer.

The admittance parameters for the device can be computed as

$$y_{ij} = \frac{I_i}{V_j} \Big|_{V_k=0, k \neq j} \quad (21)$$

where the subscripts identify the transducers in the device. Scattering parameters are then obtained from the admittance parameters by using standard transformations.

Green's Function Model

The Green's function models for SAW devices were first developed in the 1970s, with many simplifications applied at the time to make the numerical computations tractable with the resources available at the time. The most common assumption at the time was that the substrate interface was stress free (14). The technique has attracted considerable attention in recent years because of its ability to model essentially all aspects of a SAW device's performance, including taking into account the various acoustic propagation modes.

A Green's function describes the behavior of a structure subjected to a point source. This source can be an electrical charge on the surface of the substrate or a mechanical stress due to, for example, the mass of a surface electrode. In the k domain (corresponding to the Fourier transform of these terms), these relationships can be summarized as

$$\begin{bmatrix} u_1 \\ u_2 \\ u_3 \\ \phi \end{bmatrix} = \begin{bmatrix} G_{11} & G_{12} & G_{13} & G_{14} \\ G_{21} & G_{22} & G_{23} & G_{24} \\ G_{31} & G_{32} & G_{33} & G_{34} \\ G_{41} & G_{42} & G_{43} & G_{44} \end{bmatrix} \begin{bmatrix} T_{13} \\ T_{23} \\ T_{33} \\ D_3 \end{bmatrix} \quad (22)$$

where the G_{ij} terms are the Fourier transforms of the Green's functions.

A convenient method to evaluate all the Green's functions was proposed by Peach (15). For an assumed x_1 component of the acoustic wavenumber given by k_1 , the possible x_3 components can be evaluated by solving Eqs. (6)–(11). The solution can be written as an eighth-order eigenvalue problem, where the k_3 terms are the eigenvalues, and the eigenvectors are the partial waves that make up the solution. The boundary conditions determine the relative contributions of these partial waves. The G_{ij} terms are then readily obtained.

The singular terms in the G_{ij} functions must be quantified so that the Green's functions can be obtained. This step is often the most time-consuming, but it is necessary because these singular points determine the long-range effect of the sources. The Green's functions are then convolved over all sources, and the overall device behavior is obtained.

Diffraction and Beam Steering

Surface acoustic waves are generated by sources of finite aperture and are therefore subject to diffraction effects. As is done in optics, the effects are classified as near-field (Fresnel) effects and far-field (Fraunhofer) effects. In SAW devices the Fraunhofer region is of most interest.

Many of the techniques developed for optics can be applied to SAW, with the small modification that the velocity, and the wavenumber, of the waves depend on the direction of propagation. The wave velocity in a specified direction is computed by solving the stiffened Christoffel equation, as explained in (16).

A commonly used method of computing the effect of diffraction is known as the angular spectrum of waves (ASoW) technique. If we ignore any wave dependence in the x_3 direction, the amplitude of the surface wave ψ at a point (x, y) on the surface of the substrates is written (17)

$$\psi(x, y) = \int_{-\infty}^{\infty} \Psi(k_y) e^{-j(k_x x + k_y y)} dk_y \quad (23)$$

where $\Psi(k_y)$ is the Fourier transform of the wave amplitude at a reference point $x = 0$, while k_x and k_y are x_1 and x_2 components of the wavenumber for a wave propagating at an angle ϕ to the x_1 axis shown in Fig. 1. The signal detected at the receiving transducer is calculated by integrating $\psi(x, y)$ over all receiving electrodes.

Because of the anisotropy of SAW substrates, the acoustic wave front does not always propagate in the direction that is normal to the electrodes. This effect, known as beam steering, must be considered when positioning the receiving transducer.

FUTURE TRENDS

High-Velocity Surface Acoustic Waves

Commercial demand for SAW devices that can operate at high frequencies has led to a major effort to find substrates with higher acoustic velocities. Leaky waves have velocities that are about 35% higher than pure SAW, while STW and SSBW devices offer velocities that are about 60% higher than their SAW equivalents. While these modes can support higher frequencies than SAW, substrates supporting propagation modes with even higher frequencies will have to be used in the future.

A substrate that shows great promise is diamond. Since it is not piezoelectric, the diamond substrate must be in contact with a piezoelectric thin-film such as zinc oxide (ZnO). Nakahata reported that a silicon substrate coated with diamond and ZnO films can support a SAW having a velocity of 10,500 m/s and an electromechanical coupling coefficient k^2 of 1.5% (18). Diamond-based SAW devices operating well above 2 GHz should become widely available in the next few years.

New Structures

While current SAW devices can display outstanding performance in many applications, they are still limited in a number of ways. Their principal limitations are their inability to simultaneously exhibit low insertion loss and wide fractional bandwidths, and to sustain continuous high input signal power.

New structures that attempt to address these limitations continue to be developed. Wide bandwidth filters that use nonuniformly spaced transducer electrodes and reflectors show great promise, though insertion loss is inevitably sacrificed. High-power devices that distribute the acoustic power over a wider substrate surface area or that employ other acoustic modes have improved the power capability, though this is still limited to about 1 W. In addition, circuits that use a combination of SAW and leaky wave resonant structures as circuit elements in a ladder network have been shown to simultaneously improve bandwidth and power capabilities (19). Improvements in these areas can be expected in the future.

Magnetostatic Surface Waves

Magnetostatic surface wave (MSSW) devices rely on a fundamentally different physical process, but they share many similarities with SAW devices. Both employ waves that propagate on the surface of a substrate and that are generated and detected by distributed transducers. Both technologies also involve wave velocities that are several orders of magnitude slower than their electromagnetic counterparts. Magnetostatic surface waves have a low propagating loss of less than 20 dB/ μ s and a tunable velocity that permit devices operating at frequencies of up to 30 GHz (20).

An MSSW device consists of a substrate (usually sapphire, alumina, or fused silica) onto which is placed an epitaxially grown ferrimagnetic thin-film such as yttrium iron garnet (YIG). Transducers produce coupling between the RF signals and spin waves in the biased ferrimagnetic film. For wide-band devices, the transducers can consist of a microstrip line. For narrowband devices, distributed transducers consisting of meander lines or interdigital transducers can be combined with reflector gratings to produce the desired frequency response.

Three pure propagation MSSW modes can be employed: surface waves (magnetic field parallel to surface but perpendicular to wave propagation), backward volume wave (magnetic field parallel to wave propagation), and forward volume wave (magnetic field normal to surface). Each mode has its own dispersive characteristic that is controlled by both the magnetic field intensity and by the proximity of the ferrimagnetic film to a ground plane. The sensitivity to the applied magnetic field makes the devices easily tunable.

This technology has not yet found many commercial applications due to difficulties in growing high-quality ferrimagnetic thin-films, and the lack of accurate design and simulation tools.

BIBLIOGRAPHY

1. R. M. White and F. W. Voltmer, Direct piezoelectric coupling to surface elastic waves, *Appl. Phys. Lett.*, **7** (12): 314–316, 1965.

2. J. H. McClellan, T. W. Parks, and L. R. Rabiner, A computer program for designing optimum FIR linear phase digital filters, *IEEE Trans. Audio Electroacoust.*, **21** (6): 506–526, 1973.
3. R. C. Williamson and H. I. Smith, The use of surface elastic wave reflection gratings in large time-bandwidth pulse compression filters, *IEEE Trans. Microw. Theory Tech.*, **MTT-21** (4): 195–205, 1973.
4. M. Solal, P. Dufilie, and P. Ventura, Innovative SPUDT based structures for mobile radio applications, *1994 IEEE Ultrason. Symp. Proc.*, Cannes, France, 17–22, 1994.
5. H. Stark and F. B. Tuteur, *Modern Electrical Communications*, Englewood Cliffs, NJ: Prentice-Hall, 1979.
6. J. C. B. Saw, T. P. Cameron, and M. S. Suthers, Impact of SAW technology on the system performance of high capacity digital microwave radio, *1993 IEEE Ultrason. Symp. Proc.*, Baltimore, MD, 59–65, 1993.
7. R. C. Peach, F. Z. Bi, and B. van Osch, The application of surface acoustic wave filters to communications satellite design, *Proc. AIAA 15th Int. Commun. Satellite System Conf.*, California, 1994.
8. J. Machui, J. Bauregger, G. Riha, and I. Schropp, SAW devices in cellular and wireless phones, *1995 IEEE Ultrason. Symp. Proc.*, Seattle, WA, 121–130, 1995.
9. G. K. Montress, T. E. Parker, and D. Andres, Review of SAW oscillator performance, *1994 IEEE Ultrason. Symp. Proc.*, Cannes, France, 43–54, 1993.
10. P. M. Bakken and A. Rønnekleiv, SAW-based chirp Fourier transform and its application to analogue on-board signal processing, *Int. J. Satellite Commun.*, **7** (4): 283–293, 1989.
11. C. Campbell, *Surface Acoustic Wave Devices and Their Signal Processing Applications*, San Diego: Academic Press, 1989.
12. C. S. Hartmann, D. T. Bell, Jr., and R. C. Rosenfeld, Impulse response model design of acoustic surface-wave filters, *IEEE Trans. Microw. Theory Tech.*, **MTT-21** (4): 162–175, 1973.
13. Y. Xu and P. M. Smith, A theoretical and experimental study of coupled SAW resonator filters, *IEEE Trans. Ultrason. Ferroelectr. Freq. Control*, **UFFC-42** (4): 717–725, 1995.
14. D. P. Morgan, *Surface-Wave Devices for Signal Processing*, Amsterdam: Elsevier, 1991.
15. R. C. Peach, A general Green function analysis for SAW devices, *1995 IEEE Ultrason. Symp. Proc.*, Seattle, WA, 221–226, 1995.
16. B. A. Auld, *Acoustic Fields and Waves in Solids*, vol. 1, 2nd ed., Malabar: Krieger, 1990.
17. T. L. Szabo and A. J. Slobodnik, Jr., The effect of diffraction on the design of acoustic surface wave devices, *IEEE Trans. Sonics Ultrason.*, **SU-20** (3): 240–251, 1973.
18. H. Nakahata, K. Higaki, S. Fujii, A. Hachigo, K. Kitabayashi, K. Tanabe, Y. Seki, and S. Shikata, SAW devices on diamond, *1995 IEEE Ultrason. Symp. Proc.*, Seattle, WA, 361–370, 1995.
19. M. Hikita, N. Shibagaki, T. Akagi, and K. Sakiyama, Design methodology and synthesis techniques for ladder-type SAW resonator coupled filters, *1993 IEEE Ultrason. Symp. Proc.*, Baltimore, MD, 15–24, 1993.
20. W. S. Ishak and K.-W. Chang, Magnetostatic-wave devices for microwave signal processing, *Hewlett-Packard Journal*, **36** (1): 10–20, 1985.

PETER M. SMITH
McMaster University

ACOUSTIC QUANTITIES. See ACOUSTIC VARIABLES MEASUREMENT.

ACOUSTIC RESONANCE. See DEFECT ENGINEERING IN SEMICONDUCTORS USING ULTRASOUND TREATMENT.

ACOUSTICS, ARCHITECTURAL. See ARCHITECTURAL ACOUSTICS.

ACOUSTICS, UNDERWATER. See UNDERWATER ULTRASOUND.

ACOUSTIC SURFACE WAVES. See SURFACE ACOUSTIC WAVE APPLICATIONS.